

## Using Tunisian Phosphate Rock and Her Converted Hydroxyapatite for Lead Removal from Aqueous Solution

Hassen Bachoua\*, Habib Nasri\*, Mongi Debbabi\*, Béchir Badraoui\*,\*\*

\* Laboratoire de Physico-Chimie des Matériaux, Université de Monastir, Faculté des Sciences, 5019 Monastir, Tunisie.

\*\* Institut Préparatoire aux Etudes d'Ingénieur de Monastir, Université de Monastir, 5019 Monastir, Tunisie

### ABSTRACT

Natural and synthesis apatites represent a cost effective soil amendment, which can be used for in situ reduction of lead bioavailability and mobility. In our previous work, we selected Tunisian Phosphate Rock (TPR) and Hydroxyapatite (CaHAp) as promising minerals for the removal of lead from aqueous solutions. X-ray powder diffraction patterns (DRX), Infra Red (IR), Thermogravimetric analysis (TGA) and Scanning Electron Microscopy (SEM) were used to characterize TPR and CaHAp.

CaHAp was prepared from TPR and employed for the removal of  $Pb^{2+}$  ions at different concentrations from aqueous solution to determine the adsorption properties of CaHAp and compare them with those of a TPR. The kinetic data obtained indicated that the adsorption performances of the adsorbents depended both on their specific surface area and crystallinity. Complexation of lead ion on the adsorbent surface favoured the dissolution of hydroxyapatites characterized by a Ca/Pb molar ratio of 1.69. The maximum adsorption capacity of CaHAp for  $Pb^{2+}$  ions at 25 °C was 1.806 mmol /g relative to 1.035 mmol /g for TPR at the same temperature. The higher capacity of CaHAp was explained in terms of its porosity and crystallinity. The  $Pb^{2+}$  ions sorption results could be modelled by the Langmuir and Freundlich isotherms. The simulations of adsorption isotherms of  $Pb^{2+}$  on CaHAp allow us to conclude that there is a good correlation between the experimental data and the Langmuir model. On TPR, we show a good correlation between the experimental data and the Langmuir and Freundlich model.

**Index Term** - Tunisian Phosphate Rock, Hydroxyapatite, lead, sorption kinetics, Freundlich, Langmuir.

### I. INTRODUCTION

The presence of toxic heavy metal ions in industrial wastewater has caused considerable concern in recent years. The majority of studies on heavy metals (Pb, Cd, Cu ...) have shown that they are among the most toxic elements, whose toxicity can affect the nervous system, blood, bone marrow, and can also be carcinogenic to living beings. In an attempt to solve this problem, considerable efforts have been made to develop effective technologies that allow us to either remove these heavy metals or make them reach very low concentrations in industrial effluents or waters intended for living beings' consumption. Indeed, diverse new adsorbents have been developed such as hydroxyapatite, activated carbons, biomass, silica gels, Zeolites, clays, carbonaceous, and synthetic polymers [1-6]. The adsorption of heavy metals phenomenon by different materials concerns in particular, lead, cobalt, cadmium and copper. Considerable researches have been particularly done on apatites in recent years. They typically have tunnels and active surfaces responsible for the adsorption phenomenon.

Lead is one of the most widespread heavy metals present in the environment. Pb is present in the

environment in the form of highly soluble minerals such as  $PbO$ ,  $Pb(CO_3)_2$ ,  $PbSO_4$  [7]. For remediation of Pb contamination, phosphate minerals, especially apatites, were suggested [8-10]. The apatites studied include synthetic hydroxyapatite (HAp) [11-14], apatites of biological origin such as bone meal [15] and Apatite [16, 17], and phosphate rock [18-20].

In this work, we present the use of tow minerals (Tunisian phosphate Rock [TPR] and Hydroxyapatite synthesized from TPR [CaHAp]) for the removal of toxic heavy metals such as  $Pb^{2+}$ . The kinetics of the process was determined, especially in relation to the effects of various factors on the removal. The factors investigated include different  $Pb^{2+}$  concentration and contact time; Models were then developed for calculating the equilibrium metal ion concentrations at the end of each stage using the experimental Freundlich and Langmuir isotherm constants.

### II. Materials and methods

#### II.1 Adsorbents

Tow adsorbents were used in this study: Tunisian Phosphate Rock (TPR) and Hydroxyapatite synthesis from Tunisian Phosphate Rock (CaHAp). The phosphate rock sample chosen in this study originated from M'Dhilla region (Tunisia). Samples were provided by the services of Gafsa Phosphates

Company (CPG). The principal constituents of phosphate used in this study are the apatitic phases. The starting materials were washed with water, dried at 110°C overnight and sieved to give a size fraction between 100 and 400µm using ASTM sieves, according to the protocol used the research centre of CPG. The sample was crushed to obtain a homogeneous phosphate.

The hydroxyapatite (CaHAp) obtained from the Tunisian Phosphate Rock (TPR) was synthesized by a principle based on the dissolution of TPR in the nitric acid [21]. The dissolution reaction of the TPR is realized by the addition of 20 mL of nitric acid (HNO<sub>3</sub>, 65%) to 500 mL of distilled water and 30 g of PNT. The reaction mixture was stirred for 3 hours at room temperature. After filtration, the filtrate obtained is neutralized by a concentrated NH<sub>4</sub>OH solution (25 %). The pH of the reaction must be more than 10 to avoid the formation of acid phosphates. The mixture is kept in agitation for 3 hours at 90° C. The precipitate was then filtrated, washed with hot distilled water and dried at 110° C for 24 hours.

## II.2 Characterizing

X-ray diffraction analysis was carried out by means of a X'Pert Pro PANalytical diffractometer using Cu K $\alpha$  radiation ( $\lambda=1.5418 \text{ \AA}$ ), with  $\theta=0$  geometry, equipped with an X'Celerator solid detector and a Ni filter. The  $2\theta$  range was from 15 to 120° at a scanning speed of 0.0167° /minute. The thermogravimetric analysis was carried out in airflow using a TGA-DSC 1 Star system METTLER-TOLDO. Heating was performed in the range of 25° C to 1000° C. The morphology of samples was characterized using a scanning electron microscope (SEM) Zeiss Supra 55 type-VP in low voltage. The concentration of residual Pb(II) ions in the supernatant was determined by using Palintest Scanning Analyze SA1100.

## II.3 Sorption experiments

Synthetic aqueous solutions of different concentrations of lead were prepared from lead nitrate [Pb(NO<sub>3</sub>)<sub>2</sub>]. The adsorption of Lead ions on TPR and CaHAp is performed by contacting 0.2 g of the apatite studied in 100 mL of the solution of lead at 25 °C. After stirring this mixture, all adsorption experiments were carried out at an initial pH = 5. The reaction time was set at 3 hours, except for kinetic studies.

At the end of the adsorption process adsorbent was separated from the solution and supernatant was analyzed for residual Pb<sup>2+</sup> concentration by Palintest Scanning Analyze SA1100 with Precision Range 2-100 µg/l, two replicates were used for each Pb<sup>2+</sup> sorption experiments and the results given were the average values.

The adsorption capacity of TPR and CaHAp was calculated using the general equation (I): [30]

$$q_a = \frac{(C_0 - C_t)V}{m} \quad (I)$$

Where  $q_a$  is the amount of Pb<sup>2+</sup> adsorbed on TPR and CaHAp,  $C_0$  and  $C_t$  are the concentrations of metal ion (mmol/L-1) in the liquid phase initially and at time  $t$ ,  $V$  is the volume of the medium (L) and  $m$  is the amount of the TPR and CaHAp used in the reaction mixture (g).

## III. Results and discussion

### III.1 Characterization of TPR and CaHAp

#### III.1.1 DRX analysis

The figure 1 shows the powder XRD patterns of TPR (a), shows, others apatite phase, the crystalline phases such as Carbonate-Fluorapatite, Dolomite, Calcite, quartz and fluorite [15, 22,23]. The diagram associated to the powder synthesis from TPR in figure 1(b) which indicates the presence of a single phase of apatite that it is similar to the hydroxyapatite, matching well with the ICSD card #99358 for Ca<sub>5</sub>(PO<sub>4</sub>)<sub>3</sub>(OH).

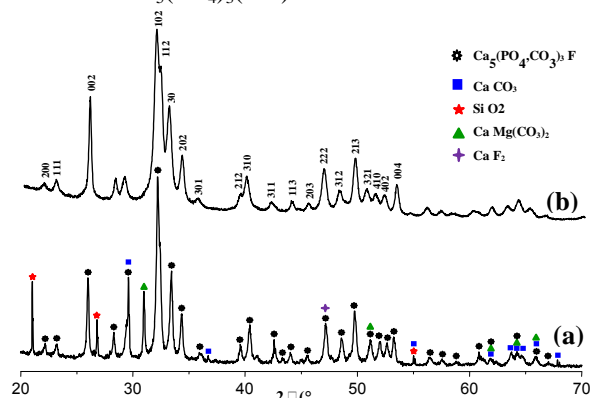


Figure 1 The XRD patterns of (a) TPR compared with that of curve of (b) CaHAp

#### III.1.2 Thermogravimetric analysis

The TGA analysis of the TPR and CaHAp curves are illustrated in figure 2(a) and 2(b). The first loss shows for CaHAp in temperature from ambient to 250°C is 2.39%, while the loss of weight of TPR in same region is 1.06%. This is due to desorption of water. When the temperature in the range of 250°C and 500°C, the curves indicated a loss of 1.03% for CaHAp, it is caused by decomposition of the carbonate ions. These carbonate ions were formed as result of CO<sub>2</sub> absorbed by the calcium phosphate [24, 25]. And loss 1.83% for TPR corresponds to the elimination of organic matter and the carbonate ions. Beyond 500°C to 1000°C, the curves shows for CaHAp a loss of 1.25% and 7.38% for TPR

correspond to decomposition of molecule water in structure and carbonate ions.

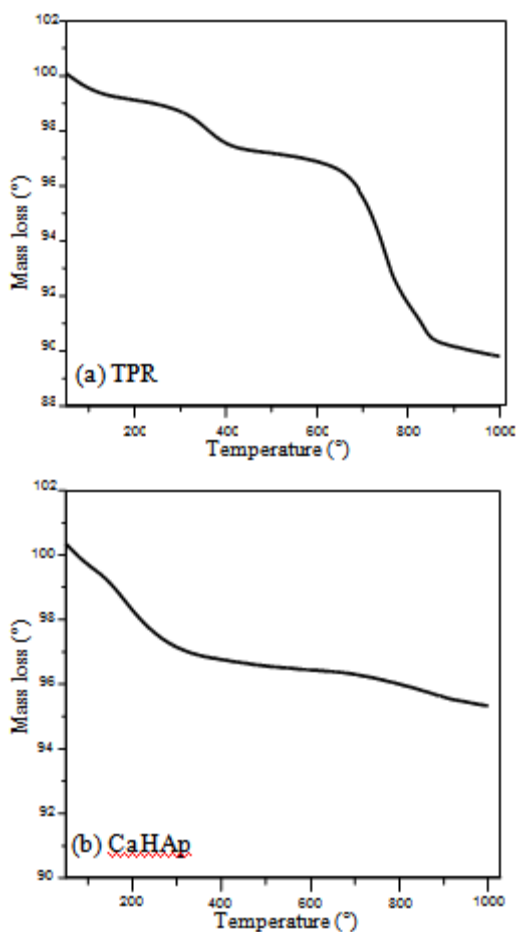


Figure 2 TGA thermogram of (a) TPR and (b) CaHAp synthesis from TPR

### III.1.3 SEM and EDX analysis

The observation under the scanning electron microscopy (SEM) (Figure 3) shows that the morphology of TPR is made mainly by particles of irregular forms, other particles, is related to the presence of the organic remainders and quartz grains. SEM analysis of CaHAp synthesis from TPR was present as aggregates, rough, granular to dense and its particles showed different shapes as short and long columns.

Coupled with the Dispersive analysis in Energy of X-rays (EDX) (Figure 4) is show the presence of Ca, P, O, Si, C, F and trace of other elements. This observation confirmed the results found by X-rays. EDX of CaHAp indicates only the presence of the elements associated to hydroxyapatite Ca, P and O, the presence of carbon due to the adsorption of CO<sub>2</sub>.

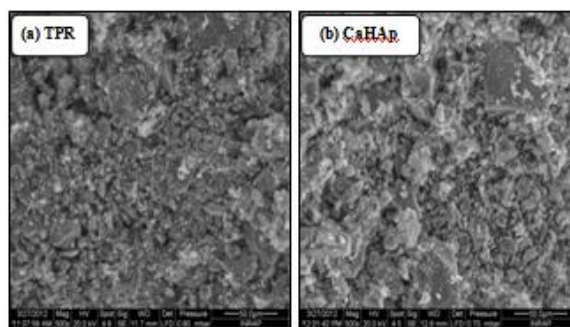


Figure 3 SEM photographs of (a) TPR and (b) CaHAp synthesis from TPR

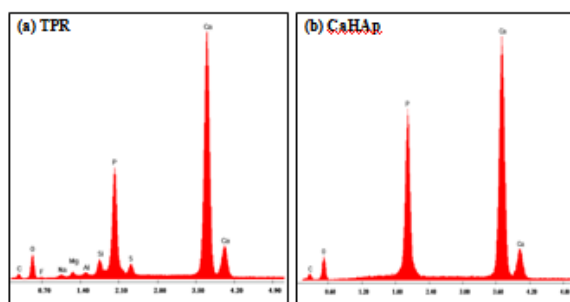


Figure 4 EDX spectra of (a) TPR and (b) CaHAp synthesis from TPR

### III.2 Sorption kinetics

Adsorption of Pb<sup>2+</sup> ions by TPR and CaHAp was measured at give contact times for three different initial Pb<sup>2+</sup> concentrations (1; 2; 4 mmol/L) illustrated in figure 5 (a) and (b).

A rapid kinetic reaction of Pb<sup>2+</sup> removal by CaHAp according in 20 min for 1 and 2 mmol/L initial concentration. While for the concentration of 4 mmol / L, it takes a longer duration (120 min) to reach this equilibrium. This difference of the time needed to equilibrium is linked firstly to the number and type of active site in the adsorbent, and the other hand to types of metal-phosphate electrostatic interactions.

Removal of Pb<sup>2+</sup> from aqueous solution by TPR shown in figure 6 indicates that take more than duration (180 min) to reach equilibrium kinetic. This longer duration is due to the low force of retention of Pb<sup>2+</sup> in the surface of TPR.

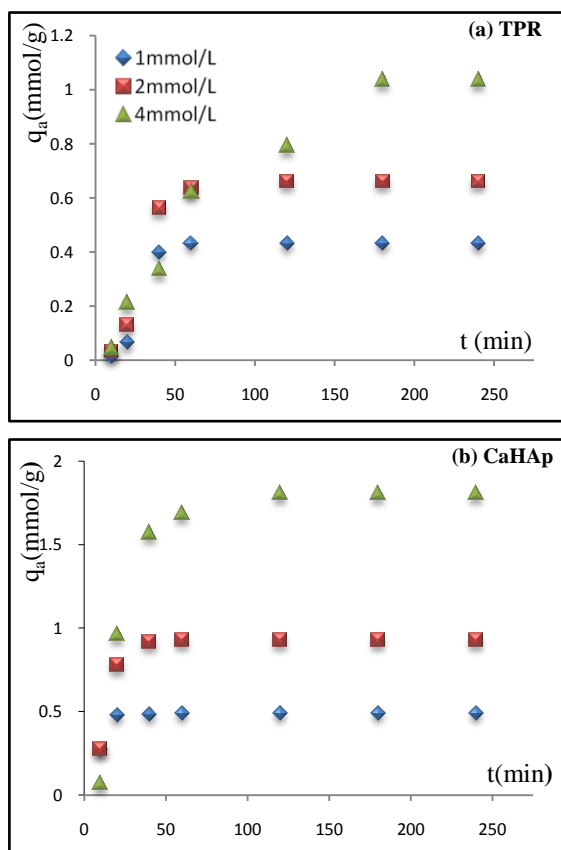


Figure 5 Effect of the initial concentration on removal of  $Pb^{2+}$  from TPR (a) and CaHAp (b)

From the results of the kinetic study illustrated by figures 5 (a) and (b), we notice that the maximum amount of  $Pb^{2+}$  ions adsorbed on the CaHAp is larger than that adsorbed on the TPR. This difference in amount of  $Pb^{2+}$  ions adsorbed by ours two powders is due to both the difference between their specific surfaces (Table 1).

Table 1 Maximum adsorption capacity of the TPR and CaHAp ( $[Pb^{2+}]_0 = 4 \text{ mmol/L}$ ,  $t = 3\text{h}$ )

| Adsorbents | $q_a$    | $Pb^{2+}$ | SS          | Ca/P |
|------------|----------|-----------|-------------|------|
|            | (mmol/g) | (%)       | ( $m_2/g$ ) |      |
| TPR        | 1.035    | 51.75     | 20.70       | 2.17 |
| CaHAp      | 1.806    | 90.30     | 47.02       | 1.69 |

### III.3 Adsorption isotherm

Figure 6 (a) and (b) illustrates the effect of the initial concentration on the removal of  $Pb^{2+}$  ions in aqueous solutions. We note that the adsorption isotherms obtained have a similar pattern, they show an increase of the adsorbed amount when the initial concentration  $Pb^{2+}$  ions is increased to a level indicating saturation of all sites on the surface of TPR and CaHAp. These adsorption isotherms are L-type according to the classification of Giles et al 1974 [26]. This suggests that the sorption process does not

only involve ion-exchange reaction but can also occur through surface dissolution, surface adsorption and precipitation [27].

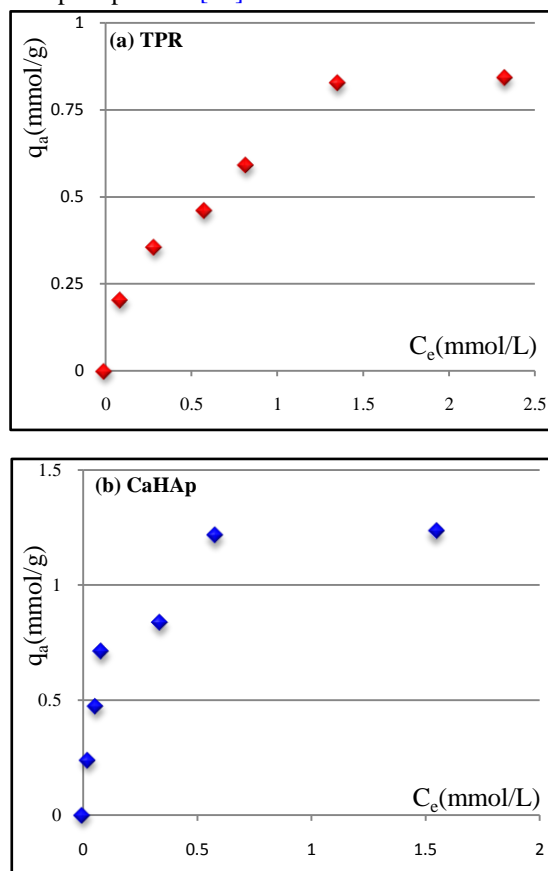


Figure 6: Effect of concentration of lead on TPR (a) and on CaHAp (b) ( $T = 25^\circ\text{C}$ ,  $pH_0 = 5$ )

### III.4 Freundlich isotherm

The Freundlich adsorption isotherm is the earliest known relationship describing the sorption equilibrium. It is in the form (II) [28]:

$$q_a = K_f C_e^{1/n_f} \quad \text{(II)}$$

Where  $q_a$  is equilibrium solid phase concentration (mmol/g),  $K$  and  $n_f$  are indicative isotherm parameters of adsorption capacity and intensity, respectively [29, 30];  $C_e$  is equilibrium liquid phase concentration (mmol/L). The well-known logarithmic form Freundlich isotherm is given by the following equation (III):

$$\text{Log } C_a = \text{Log } K_f + \frac{1}{n_f} \text{Log } C_e \quad \text{(III)}$$

In this equation,  $1/n_f$  represents the gradient of the straight. When this ratio  $1/n$  is equal to unity, this means that there is a constant distribution of solute between the adsorbent and the liquid phase. In the case of curves for apatites that have values  $1/n_f$  different from unity, the corresponding isotherms are not linear, indicating that it becomes increasingly difficult for a molecule or ion to find a Site adsorbent

available. The adsorption coefficient  $K_f$  translates the adsorptivity of an adsorbent for a given adsorbate.

Representation of  $\text{Log } q_a$  depending to  $\text{Log } C_e$  relating TPR and CaHAp give two lines (Figures 7 (a) and (b)). The equations for the two curves obtained are:

-TPR:  $\text{Log } q_a = 0.465 \text{ Log } C_e - 0.466$  (IV)

With  $R^2 = 0.979$

-CaHAp:  $\text{Log } q_a = 0.370 \text{ Log } C_e + 0.247$  (V)

With  $R^2 = 0.862$

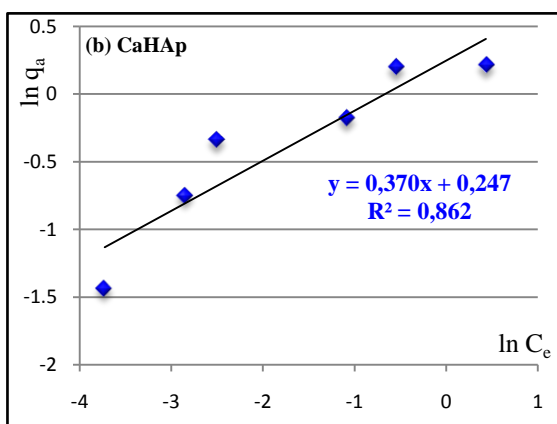
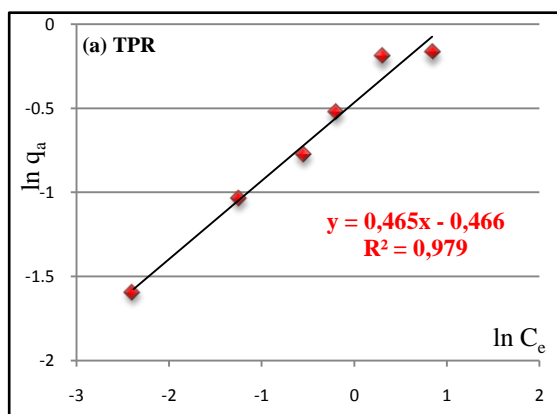


Figure 7 Freundlich isotherm plot for the adsorption of  $\text{Pb}^{2+}$  ions by TPR (a) and CaHAp (b)

### III.4 Langmuir isotherm

It is the most widely used to model the results found during the adsorption of heavy metals in aqueous solution.

It is not theoretically applicable in the case of adsorption sites localized, homogeneous and without lateral interactions between the adsorbed particles. It also indicates that the adsorption reaction is reversible.

The Langmuir model thus based on the existence of a dynamic equilibrium between the entities that bind and those that leave the surface. This can be defined by the following equilibrium equation (VI) [31]:

$$q_a = \frac{b \cdot q_m \cdot C_e}{1 + b \cdot C_e} \quad \text{(VI)}$$

The linearization of the above equation leads to the following relationship (VII):

$$\frac{C_e}{q_a} = \frac{1}{b \cdot q_m} + \frac{C_e}{q_m} \quad \text{(VII)}$$

where  $q_a$  is the equilibrium adsorption capacity of adsorbent (mmol/g),  $C_e$  is the equilibrium concentration of metal ions (mmol/L),  $q_m$  is the maximum amount of metal ions adsorbed (mmol/g), and  $b$  is the constant that refers to the bonding energy of adsorption (L/mmol). The constants  $b$  and  $q_m$  can be determined from the intercept and slope of the linear plot  $C_e/q_a$  versus  $C_e$ .

Linear representation of the experimental values of the adsorption of ions  $\text{Pb}^{2+}$  by TPR and CaHAp studied claimed to the Langmuir model are illustrated in figures 8 (a) and (b).

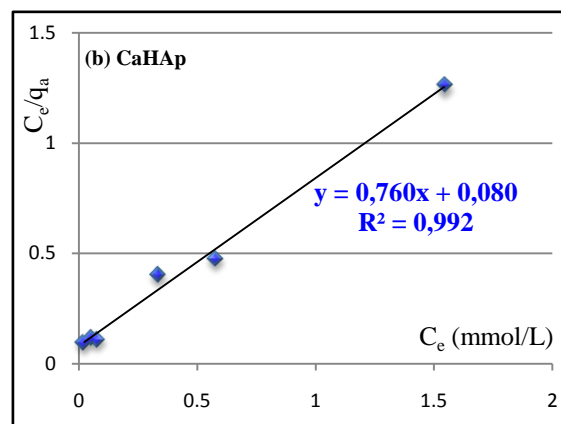
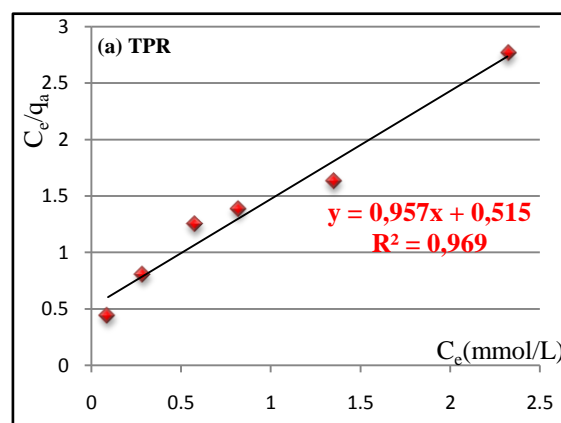


Figure 8: Langmuir isotherm plot for the adsorption of  $\text{Pb}^{2+}$  ions by TPR (a) and CaHAp (b)

Due to an adjustment by the least square method, we obtain for each studied law and for TPR and CaHAp tested lines with which various constants were derived and are summarized in table 2.

Table 2 Freundlich and Langmuir constants and correlation coefficients for adsorption of  $\text{Pb}^{2+}$  on TPR and CaHAp.

| Adsorbent | Freundlich |         |       | Langmuir |       |       |
|-----------|------------|---------|-------|----------|-------|-------|
|           | $k_f$      | $1/n_f$ | $R^2$ | $q_m$    | $b$   | $R^2$ |
| TPR       | 0.627      | 0.465   | 0.979 | 1.045    | 1.858 | 0.969 |
| CaHAp     | 2.368      | 0.370   | 0.862 | 1.316    | 9.500 | 0.992 |

Based on the correlation coefficients ( $R^2$ ) relative to the straight linearity of the adsorption isotherms of the two models, we can conclude that the Freundlich model is most likely to characterize the adsorption of ions  $Pb^{2+}$  on both types of adsorbents. The capacity values of the monomolecular  $q_m$  coincide with those of the experimental highest adsorbed amount of lead ions in the data table X, This shows that CaHAp has a high affinity with respect to ions  $Pb^{2+}$ . Table 3 gives comparative equilibrium capacities ( $q_m$ ) of lead ion on various adsorbents. The result reveals that TPR and CaHAp were effective in attenuating lead in aqueous solution.

Table 3 Comparison of adsorption capacities for  $Pb^{2+}$  between different adsorbents.

| Adsorbent         | $q_m$ (mmol/L) | Reference |
|-------------------|----------------|-----------|
| TPR               | 1.045          | This work |
| CaHAp             | 1.316          | This work |
| CaHAp             | 0.410          | [32]      |
| Natural phosphate | 0.555          | [19]      |
| CHAp              | 0.455          | [33]      |
| Phosphatic clay   | 0.179          | [20]      |

### III.5 Simulation of the adsorption isotherm

After obtaining all the experimental results and established the adsorption isotherms of ions  $Pb^{2+}$  about the two types of adsorbents. We have undertaken to systematically simulate all the experiences we have made by both Langmuir and Freundlich to search and confirm the best representation of the experimental points from these models. The experimental points simulated using equations Langmuir and Freundlich indicating the variation of the adsorbed quantity ( $q_a$ ) of  $Pb^{2+}$  ions of CaHAp and TPR depending on the residual concentration of the solution at equilibrium ( $C_e$ ) are shown in figures 13 and 14. These results show that for  $Pb^{2+}$  ions is on the agreement between simulation and experiment is acceptable.

Indeed, the simulation curves of adsorption isotherms of  $Pb^{2+}$  on CaHAp allow us to conclude that there is a good correlation between the experimental data and the Langmuir model. This indicates the formation of a monomolecular covering of the surface sites of CaHAp. For TPR, the simulation curves of adsorption isotherms of  $Pb^{2+}$  shows a good correlation between the experimental data and the Freundlich and Langmuir model.

These simulation results are confirmed by the Langmuir constants listed in the table 2 and are determined graphically after linearization of the equation of this model.

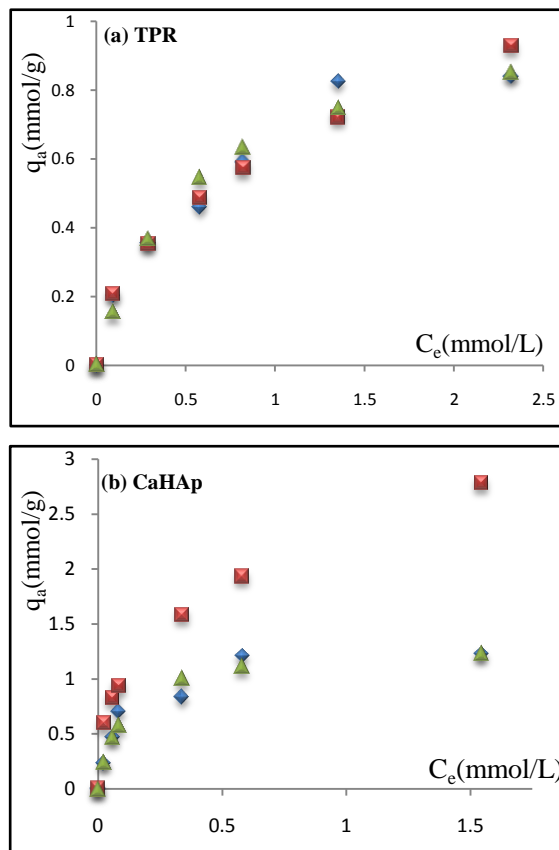


Figure 9 Langmuir and Freundlich models for the lead adsorption isotherm by TPR (a) and CaHAp (b)

### IV. Conclusion

After successfully synthesize hydroxyapatite (CaHAp) from the Tunisian phosphate rock (TPR), the comparative study of  $Pb^{2+}$  ions adsorption on these two showed the effect of the specific surface of the material used.

This study showed that CaHAp is an appropriate and effective for the adsorption of  $Pb^{2+}$  aqueous solutions relative to a TPR. This is a consequence of the lower crystallinity and higher porosity of the former with respect to the latter material. The Langmuir isotherm model fitted the experimental equilibrium data reasonably well and was found to be superior to the Freundlich model. The maximum uptake capacity of  $Pb^{2+}$  was 1.806 mmol /g for CaHAp and 1.035 mmol /g for TPR.

### V. Acknowledgments

We are thankful to Gafsa Phosphates the Company (GPC-CPG) for providing the investigated phosphate sample, the (RTCEn) Research and Technology Centre for Energy and the University of Monastir (Tunisia). Thanks are also expressed to Prof

J-Marie Nedelec and Prof Guillaume Renaudin, (teams PMB) Institute of Chemistry of Clermont-Ferrand.

## References

- [1] A. Aklil, M. Mouflih, S. Sebti, *Removal of heavy metal ions from water by using calcined phosphate as a new adsorbent, J. Hazard. Mater*, 112, 2004, 183-190.
- [2] M. Mouflih, A. Aklil, S. Sebti, *Removal of lead from aqueous solutions by activated phosphate, J. Hazard. Mater*, 119, 2005, 183-188.
- [3] M. Machida, R. Yamazaki, M. Aikawa, H. Tatsumoto, *Role of minerals in carbonaceous adsorbents for removal of Pb(II) ions from aqueous solution, Sep. Purif. Technol*, 46, 2005, 88-94.
- [4] K.S. Hui, C.Y.H. Chao, S.C. Kot, *Removal of mixed heavy metal ions in wastewater by zeolite 4A and residual products from recycled coal fly ash, J. Hazard. Mater*, 127, 2005, 89-101.
- [5] Y. Bulut, Z. Baysal, *Removal of Pb(II) from wastewater using wheat bran, J. Environ. Manage*, 78, 2006, 107-113.
- [6] G. Issabayeva, M.K. Aroua, N.M.N. Sulaiman, *Removal of lead from aqueous solutions on palm shell activated carbon, Bioresour. Technol*, 97, 2006, 2350-2355.
- [7] X. Cao, L.Q. Ma, S.P. Singh, O. Zhou, *Phosphate-induced lead immobilization from different lead minerals in soils under varying pH conditions, Environ. Pollut*, 152, 2008, 184-192.
- [8] T. Suzuki, K. Ishigaki, N. Ayuzawa, *Removal of toxic Pb<sup>2+</sup> ions by synthetic hydroxyapatites, Chem. Eng. Commun.* 34, 1985, 143-151.
- [9] Q.Y. Ma, S.J. Traina, T.J. Logan, J.A. Ryan, *In situ lead immobilization by apatite, Environ. Sci. Technol*, 27, 1993, 1803-1810.
- [10] A.S. Knox, D.I. Kaplan, M.H. Paller, *Phosphate sources and their suitability for remediation of contaminated soils, Sci. Tot. Environ*, 357, 2006, 271-279.
- [11] M. Manecki, P.A. Maurice, S.J. Traina, *Kinetics of aqueous Pb reaction with apatites, Soil Sci*, 165, 2000, 920-933.
- [12] S. Baillez, A. Nzihou, D. Bernache-Assolant, E. Champion, P. Sharrock, *Removal of aqueous lead ions by hydroxyapatites: equilibria and kinetic processes, J. Hazard. Mater*, 139, 2007, 443-446.
- [13] Y. Hashimoto, T. Sato, *Removal of aqueous lead by poorly-crystalline hydroxyapatites, Chemosphere*, 69, 2007, 1775-1782.
- [14] H.Y. Xu, L. Yang, P. Wang, Y. Liu, M.S. Peng, *Kinetic research on the sorption of aqueous lead by synthetic carbonate hydroxyapatite, J. Environ. Manage.* 86 (2008) 319-328.
- [15] B. Perdikatsis, *X-ray powder diffraction study of francolite by the Rietveld method, Materials Science Forum* 79, 1991, 809-814.
- [16] J.L. Conca, *Phosphate-Induced Metal Stabilization (PIMS), Final Report to the U.S. Environmental Protection Agency #68D60023, U.S. Environmental Protection Agency, Research Triangle Park, 1997.*
- [17] J.L. Conca, J. Wright, *An apatite II permeable reactive barrier to remediate groundwater containing Zn, Pb and Cd, Appl. Geochem*, 21, 2006, 1288-1300.
- [18] E. Mavropoulos, N.C.C. da Rocha, J.C. Moreira, L.C. Bertolino, A.M. Rossi, *Pb<sup>2+</sup>, Cu<sup>2+</sup> and Cd<sup>2+</sup> ions uptake by Brazilian phosphate rocks, J. Braz. Chem. Soc*, 16, 2005, 62-68.
- [19] M. Mouflih, A. Aklil, N. Jahroud, M. Gourai, S. Sebti, *Removal of lead from aqueous solutions by natural phosphate, Hydrometallurgy*, 81, 2006, 219-225.
- [20] S.P. Singh, L.Q. Ma, W.G. Harris, *Heavy metal interactions with phosphatic clay: sorption and desorption behavior, J. Environ. Qual.* 30, 2001, 1961-1968.
- [21] S. El Asri, A. Laghzizil, A. Alaoui, A. Saoiabi, R. M'Hamdi, K. El Abbassi, A. Hakam, *Structure and thermal behaviours of Moroccan phosphate rock (Bengurir). Journal of Thermal Analysis and Calorimetry*, 95 (1), 2009, 15-19.
- [22] W. Zheng, X.M. Li, Q. Yang, G.M. Zeng, X.X. Shen, Y. Zhang, J.J. Liu, *Adsorption of Cd(II) and Cu(II) from aqueous solution by carbonate hydroxyapatite derived from eggshell waste, J. Hazard. Mater*, 147, 2007, 534-539.
- [23] H. Bachouâ, M. Othmani, Y. Coppel, N. Fatteh, M. Debbabi, B. Badraoui, *J. Mater. Environ. Sci*, 5, 2014, 1152-1159.
- [24] S. P. Parthiban, K. Elayaraja, E. K. Girija, Y. Yokogawa, R. Kesavamoorthy, M. Palanichamy, K. Asokan, S. Narayana Kalkura, *Preparation of thermally stable nanocrystalline hydroxyapatite by hydrothermal method, J Mater Sci: Mater Med*, 20, 2009, 77-83.
- [25] F. G. Correa, J. B. Martinez, J. S. Gomez, *synthesis and characterization of calcium phosphate and its relation to cr(vi) adsorption properties, Revista internacional de contaminación ambiental*, 26, 2010, 129-136.

- [26] C.H. Giles, D. Smith, A. Huitson, *A general treatment and classification of the solute adsorption isotherm. I. Theoretical*, *J. Colloid. Interf. Sci.* 47, 1974, 755-765.
- [27] S.H. Jang, B.G. Min, Y.G. Jeong, W.S. Lyoo, S.C. Lee, *Removal of lead ions in aqueous solution by hydroxyapatite/polyurethane composite foams*, *J. Hazard.Mater.*, 152, 2008, 1285–1292.
- [28] H.M.F. Freundlich, *over the adsorption in solution*, *J. Phys. Chem.*, 57, 1906, 385–470.
- [29] E. Malkoc, Y. Nuhoğlu, *The removal of chromium. (VI) From synthetic wastewater by Ulothrix zonata*, *Fresenius Environ. Bull.*, 12, 2003, 376-381.
- [30] K. Kadirvelu, K. Thamarai Selvi, C. Namasivayam, *Adsorption of nickel(II) from aqueous solution onto activated carbon prepared from coirpith*, *Sep. Purif. Technol.* 24, 2001, 497-505.
- [31] I. Langmuir, *The constitution and fundamental properties of solids and liquids. Part I. Solids*, *J. Am. Chem. Soc.*, 38, 1946, 2221–2295.
- [32] A. Yasukawa, T. Yokoyama, K. Kandori, T. Ishikawa, *Reaction of calcium hydroxyapatite with Cd<sup>2+</sup> and Pb<sup>2+</sup> ions*, *Colloids Surf. A: Physicochem. Eng. Aspects*, 299, 2007, 203–208.
- [33] L. Dexiang, Z. Wei, L. Xiaoming, Q. Yang, Y. G. Xiu, Z. Liang, Guangming, *Removal of lead(II) from aqueous solutions using carbonate hydroxyapatite extracted from eggshell waste*, *Journal of Hazardous Materials*, 177, 2010, 126–130.